DOI: 10.1002/ejic.201000126

Europium Complexes of Tris(dipicolinato) Derivatives Coupled to Methylumbelliferone: A Double Sensitization

Julien Andres[a] and Anne-Sophie Chauvin*[a]

Dedicated to Professor Jean-Claude Bünzli on the occasion of his 65th birthday

Keywords: N, O ligands / Lanthanides / Luminescence / Europium / Sensitization

A *para*-poly(oxyethylene) dipicolinic acid derivative coupled to methylumbelliferone was synthesized and used as a ligand for coordination with europium ions. Characterization of the complex by mass spectrometry and spectrophotometry was performed in aqueous solution and points to the formation of the 1:3 Eu/L complex. Physicochemical properties are close to those of already reported dipicolinato complexes, confirming that the presence of a coumarin chromophore does not interfere with complex formation. Photophysical measurements result in observed lifetimes of 1.4 ms and intrinsic quantum yields, Φ_{Eu}^{Eu}, ranging from 33 to 50 % (depending on the solvent used). Selective excitation can be performed either mostly on the dipicolinate (DPA) backbone (at 280 nm) or exclusively on the coupled coumarin chromophore in the near visible range (320 nm). Despite the spatial distance between the antenna and the lanthanide ion, europium emission was observed upon 320 nm excitation together with the coumarin emission. The different sensitization pathways have been explored and rationalized. Finally, the complex has been used to probe the ratio of a binary mixture of solvent, establishing the potential interest of this new class of ligands in many fields of research, from photophysics to applied chemistry.

Introduction

2,6-Pyridinedicarboxylic acid, also known as dipicolinic acid (DPA) or dipic, is a well-known framework in lanthanide coordination chemistry, which forms stable complexes[1,2] with interesting luminescence properties. The structures of these complexes have been deduced by using X-ray diffraction analysis[3–6] and by analysis of the lanthanide-induced shifts (LIS).[7–10] This small ligand provides a good sensitization of most of the lanthanide ions, with a particularly high quantum yield for the europium and terbium complexes,[11] the sensitization occurring through the dipic^{2-} triplet state[12] (with an efficiency of 85 % in the solid state[13] and 61 % in solution[11]). Apart from the parent dipic compound, the pyridine ring can be functionalized, in particular at its *para* position, the influence of the grafted substituent being well documented by several authors.[14–19] These couplings have often resulted in a decrease in luminescence efficiency relative to dipicolinic acid, due to a mismatch of the triplet states of the complexed ligands with the excited states of the lanthanides. However, promising results have also been achieved with substantial increase in overall quantum yields.[20,21] Near-infrared luminescence from Nd^{III}, Dy^{III}, Er^{III}, Tm^{III}, and Yb^{III} is also sensitized by dipicolinate moieties,[9,22,23] although usually to a lesser extent than visible emission. For all these reasons, this family of complexes was used in several applications, such as various inorganic–organic hybrid materials,[24] nanoparticles,[25] or as analytical probes, particularly for the analysis of bacterial spores[26–28] or of nanomolar concentrations of Tb^{III}.[29] Finally, lanthanide dipicolinates display nonlinear optical (NLO) properties[30,31] and two-photon excitation luminescence, either through an allowed Tb^{III} f–f transition[32] or through the ligand,[33,34] enabling luminescence microscopy images to be collected under NIR excitation. Despite these extensive studies and applications developed with dipic complexes, the potentialities of these kinds of ligands still have to be extended, and several routes can be exploited to improve their capability as luminescent markers. Above all, dipicolinic acid has a maximum of excitation that is limited to the UVC region (λ_{max} = 280 nm), and extending it to the near visible region is of importance. Recently, coupling polyoxyethylene dipicolinic acid derivatives with biological materials has been successfully undertaken.[18,35] The presence of a polyoxyethylene chain at the fourth position of the pyridine ring has been shown to slightly affect the coordination ability of dipicolinic acid derivatives relative to their non-polyoxyethylene analogs and has demonstrated an interesting fine tuning of the lumines-

[a] École Polytechnique Fédérale de Lausanne, ISIC, BCH 1405, 1015 Lausanne, Switzerland
E-mail: anne-sophie.chauvin@epfl.ch
julien.andres@epfl.ch

Supporting information for this article is available on the WWW under http://dx.doi.org/10.1002/ejic.201000126.

cence properties depending on the coupled molecule at the extremity of the polyoxyethylene chain.[18] This change in luminescence properties is not straightforward, even if some of the results can be rationalized by the introduction of known quenching functional groups such as free alcohol or amine groups.

Motivated by these interesting results, we decided to attach chromophores or fluorophores at the end of the polyoxyethylene chain in order to test whether we could sensitize lanthanide ions through space with an uncoordinated chromophore. The presence of two different chromophores, the dipicolinate moiety, and the additional coupled chromophore provides an unusual and novel challenge in understanding the photophysics of luminescent lanthanide complexes. Furthermore, the interaction of the two chromophoric units with each other and with the lanthanide ion might find some useful applications in various domains, from bioimaging to color reproduction. The choice of the second chromophore was critical. The first requirement was that it had to absorb at higher wavelengths than the dipicolinic moiety, whose absorption occurs below 300 nm. On the other hand, the absorption had to remain in the UV range to ensure that the emission would be not too far away from the europium and terbium emissive excited states. Simple coumarin derivatives, which have absorptions below 380 nm and emission maxima around 400 nm, have been found to be good candidates. Moreover, a well-documented effect of the substitution of these derivatives relative to the effect on the fluorescence emission is available in the literature, allowing a fine tuning of the emission and absorption maxima.[36–38] Due to its commercial availability, low price, and matching photophysical properties, the candidate chosen first was 4-methylumbelliferone (4-methyl-7-hydroxycoumarin), coupled through its 7-hydroxy group (Figure 1). In such structures, the maximum distance between the Eu^{3+} ion and the coumarin chromophore is around 17 Å. We report here the synthesis of *para*-polyoxyethylene dipicolinic acid derivatives coupled to methylumbelliferone as ligand for luminescent lanthanide ions. The photophysical properties of the europium complex both in aqueous solution and in the solid state will be described in an attempt to rationalize the mode of sensitization by these new types of ligands.

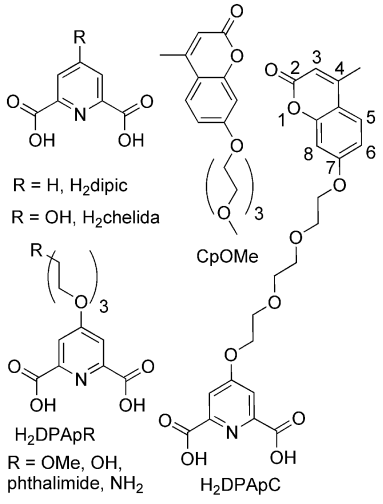

Figure 1. Ligands derived from dipicolinic acid.

Results and Discussion

Synthesis of the Ligand and Its Europium Complex

The strategy used to synthesize ligand H_2DPApC is described in Figure 2. Coupling the coumarin chromophore to a methoxypolyoxyethylene chain is first achieved by reacting methylumbelliferone (**1**) with brominated methoxypolyoxyethylene chain **2** obtained from the alcohol derivative. The methoxy group of the CpOMe chromophore is then removed by TMSI (trimethylsilyl iodide) to yield free alcohol **3**. Coupling of **3** with diethyl chelidamate (**4**) is undertaken through a Mitsunobu reaction. The last step consists of a deprotection of the carboxylic acid moieties of **5** to yield ligand H_2DPApC. The global yield of the reaction is 45%. The sodium salt of the ligand is water-soluble; it is mixed with europium(III) perchlorate in a 1:3 Eu/L ratio to form europium complex $[Eu(DPApC)_3]^{3-}$.

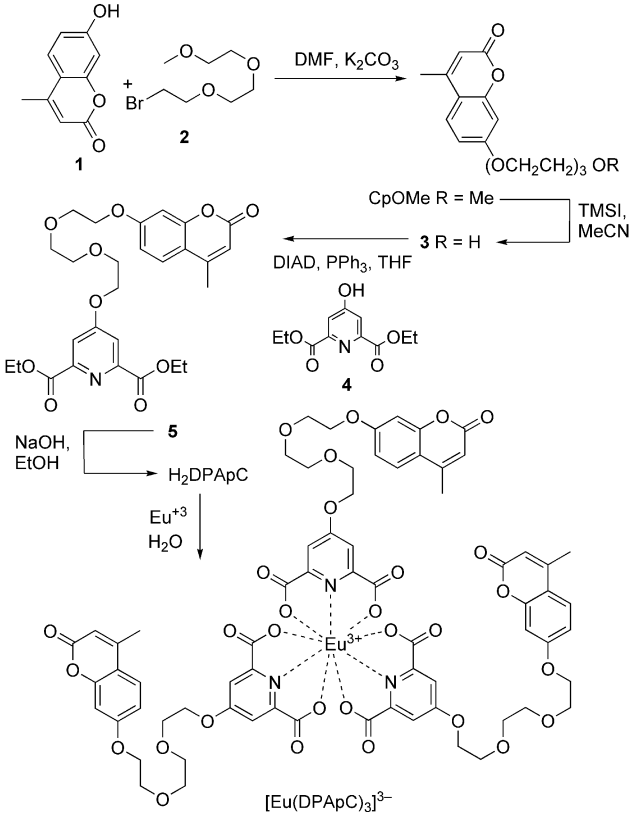

Figure 2. Synthetic strategy for the synthesis of ligand H_2DPApC and its europium complex $[Eu(DPApC)_3]^{3-}$.

Stoichiometry and Stability of the Ln Complexes

Mass Spectrometry of the Europium Complex

In order to confirm the formation of a major amount of $[Eu(DPApC)_3]^{3-}$ complex in 1:3 stoichiometry, a sample of

concentration 1×10^{-4} M in Eu^{3+} and 3×10^{-4} M in ligand was examined by mass spectrometry with electron spray ionization in the negative mode. The experiment shows series of peaks consistent with the 1:3 stoichiometry of the desired complex $[Eu(DPApC)_3]^{3-}$: half the exact mass of the monoprotonated complex ($[Eu(DPApC)_3]^{3-}$, m/z = 783.67) and half the exact mass of the monoprotonated complex with a water molecule ($\{[Eu(DPApC)_3]^{3-} + H_2O\}$, m/z = 792.68, see Supporting Information, Figure S1).

Emission and Absorption As a Function of Europium-to-Ligand Ratio

The stability of the complex is often critical for good luminescence properties. In the case of 1:3 complexes such as dipicolinato derivatives, 1:2 and 1:1 species have poor luminescence due to the quenching by water molecules in the first coordination sphere. The appearance of these species at higher than 1:3 stoichiometries thus decreases the emission intensity of the luminescent lanthanide ion. Monitoring the intensity of the europium emission as a function of europium-to-ligand ratio hence allows observing the emergence and vanishing of the species with the strongest luminescence (the 1:3 species). The excitation wavelength was chosen at the coumarin absorption maximum, that is, 320 nm. This wavelength would also allow monitoring the emission intensity of the coumarin moiety as a function of ligand-to-europium ratio. Complexation with europium ion might indeed alter the coumarin emission. A titration of a 3×10^{-4} M solution of the ligand with increasing amounts of europium perchlorate were undertaken. The pH value of the solution was set at 7.4 with a Tris buffer, in a manner similar to other studies with dipicolinato complexes. Figure 3 shows the emission intensity of the coumarin and sensitized emission from europium upon addition of europium perchlorate. The emission of europium exhibits a nice bell-shaped curve with a maximum in the presence of 0.3 equiv. Eu^{3+}. On the other hand, the coumarin emission resembles a sigmoid with a constant emission starting from 0.33 equiv. europium ions. These results are then consistent with the formation of a luminescent 1:3 complex under stoichiometric conditions. Additionally, formation of a precipitate above 0.66 equiv. was observed. The absorbance of the ligand was also monitored as a function of the amount of Eu^{3+} (Supporting Information, Figure S2), but precipitation did occur above 0.66 equiv. Eu^{3+}, so that no stability constant data could be extracted from these experiments and hence no correlation can be established with the dipic ligand. However, according to previous results for DPApR ligands,[18] it was established that stability constants of the Eu complexes were close to those of dipic. It seems then reasonable to consider that the DPApC ligand has the same lanthanide complexation ability.

Emission as a Function of pH

Dealing with luminescent materials in aqueous solution requires finding out the optimum pH values. In order to establish the best conditions for luminescence, the emission spectrum of an aqueous solution of $[Eu(DPApC)_3]^{3-}$ was monitored as a function of pH. Two excitation wavelengths were chosen. The first one at 280 nm is centered on the absorption of the DPA and coumarin moieties. The second one at 320 nm is at the absorption maximum of the coumarin chromophore, where DPA does not absorb any light. The emission of the coumarin moiety has a maximum at 389 nm. Upon excitation at 280 nm, its intensity slightly increases as pH increases from 2.5 to 10.4. On the other hand, upon excitation at 320 nm, a significant increase of 175% in intensity is observed. In parallel, the emission intensity of the europium ion is higher when excited at 280 nm rather than at 320 nm. All these results confirm that coumarin is highly emissive at λ_{ex} = 320 nm, whereas the luminescence of europium is more intense than that of coumarin at λ_{ex} = 280 nm.

Above pH 6.3, the difference in intensity between 280 and 320 nm excitation is quite constant and close to a ratio of 1.8. This is also dependent on the pH (Figure 4). Below pH 6, the ratio is not constant anymore, reflecting that coumarin emission is less affected by a fairly acidic medium,

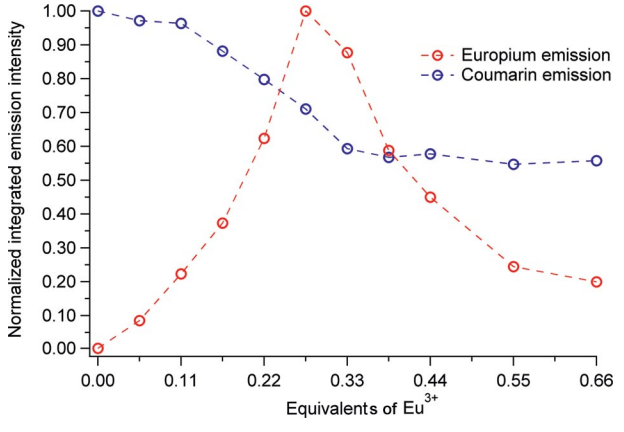

Figure 3. Normalized integrated emission of europium (red) and coumarin (blue) emission upon 320 nm excitation and upon addition of europium perchlorate to a 3×10^{-4} M solution of $(DPApC)^{2-}$ in Tris (0.1 M, pH 7.4).

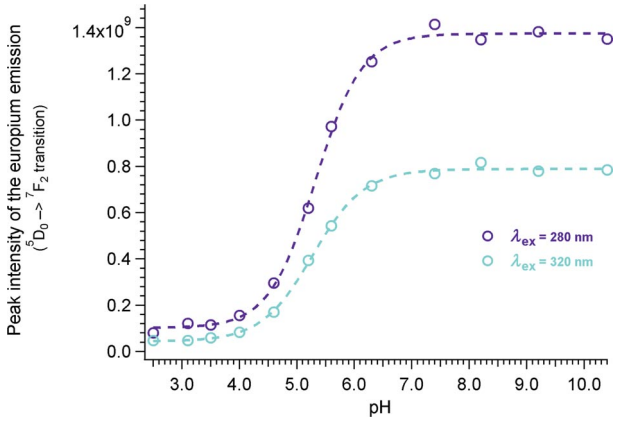

Figure 4. Peak intensity of the $[Eu(DPApC)_3]^{3-}$ $^5D_0 \rightarrow {}^7F_2$ transition in aqueous solution as a function of pH.

whereas europium emission depends on the stability of the complex (with competition between complexation and protonation of the carboxylic acid functions at low pH values). For comparison with already reported results within this series, we fixed the pH at 7.4 (by means of Tris buffer solution) for all the following experiments.

Emission Spectrum of the $[Eu(DPApC)_3]^{3-}$ Complex

The emission spectrum of the $[Eu(DPApC)_3]^{3-}$ complex has the same shape as those of other DPApR complexes where R = OH, NH_2, OMe, or phthalimide[18] (Figures 7 and S3), with the same relative intensities, so that it can be established that the coordination spheres around the europium cation are equivalent for all the dipicolinato ligands. This also indicates that the presence of the coumarin moiety does not interfere with the coordination sphere.

Furthermore, lifetime measurements both in water, $\tau_{obs}(H_2O) = 1.4 \pm 0.1$ ms, and in deuteriated water, $\tau_{obs}(D_2O) = 2.6 \pm 0.1$ ms, lead to the conclusion that no water molecule is in the first coordination sphere ($q = 0.02$), by using the Horrocks phenomenological relations [Equations (8) and (9) in the Experimental Section] with $\alpha = 0.31$ ms^{-1} and $A = 1.11$ ms, and zero XH oscillators in the first coordination sphere.[39] This last result confirms that the coordination sphere of the europium ion is filled by the three tridentate dipicolinate entities, the lifetimes obtained being close to those previously obtained within the dipicolinato series.

High-Resolution Excitation of the $^5D_0 \rightarrow {}^7F_2$ Transition

A high-resolution excitation spectrum was measured on the powder solid sample at 12 K by direct excitation on the $^5D_0 \leftarrow {}^7F_0$ transition. The emission intensity of the $^5D_0 \rightarrow {}^7F_2$ transition at 615 nm was monitored as a function of the excitation wavelength. The resulting spectrum (Figure S4) shows a single peak located at 17223 cm^{-1} (580.61 nm) with a half-width of 17.9 cm^{-1}. Hence, only one europium geometry is present in the solid-state sample, which is in all probability similar to that of $Cs_3[Eu(dipic)_3]$ (D_3 symmetry). All these results are in agreement with the hypothesis of the similarity between the coordination of the europium ion to DPApC ligands and that to DPApR or dipic ligands.

Photophysical Properties

Luminescence of the Uncoupled Chromophore CpOMe

To begin with, the luminescence properties of the free methoxypolyoxyethylene coumarin chromophore CpOMe (Figure 1) were measured in aqueous solution [saturated aqueous solution diluted ten times in Tris (0.1 M, pH 7.4)] and in the solid state. The addition of the polyoxyethylene chain ensures that the chromophore is in the same conformation as it is once coupled to DPA. Indeed, the uncoupled 4-methylumbelliforone can exist in different protonation states depending on the pH (pK_a of the 7-OH group is around 7.4), different tautomeric forms, or different charged structures.[40] Most of these properties are due to the acidic proton at the 7th position. Hence, coupling with the polyoxyethylene chain removes part of the complexity of the coumarin behavior that comes from this proton. The excitation and absorption spectra in Tris (0.1 M pH 7.4) aqueous solution (Figure S5) show good overlap once normalized, with a maximum absorption at 320 nm and absorption up to 360 nm. Fitting of the molar extinction coefficients with Gaussian peaks (Figure S6) is achieved with three Gaussian peaks centered at 291 nm, 320 nm, and 336 nm. As it will be shown later, these three peaks can be attributed to π–π* and n–π* transitions.

On the other hand, the excitation spectrum in the powder solid state is quite different from that in solution (Figure 5). The shape is broader with local maxima at 275 nm and 353 nm, with a curvature in between, and a shoulder around 390 nm. As a consequence, excitation can take place at higher wavelength in the solid state, up to 400 nm, whereas in solution, excitation only up to 360 nm is possible. This additional band with a local maximum at 353 nm is certainly due to intermolecular interaction in the solid state. The shape of the spectrum is hence very different in the solid state, because of all the important changes in the surroundings of the molecules once the solvent is removed. The three peaks fitted in Figure S6 are thus hidden in the broad structure of the solid-state excitation spectrum. The peak at 291 nm may appear with a slight hypsochromic shift in the solid state at 275 nm, whereas the other two are less well-defined. Additionally, the excitation below 300 nm is much more efficient in the solid state with a maximum at 275 nm relative to 320 nm in solution.

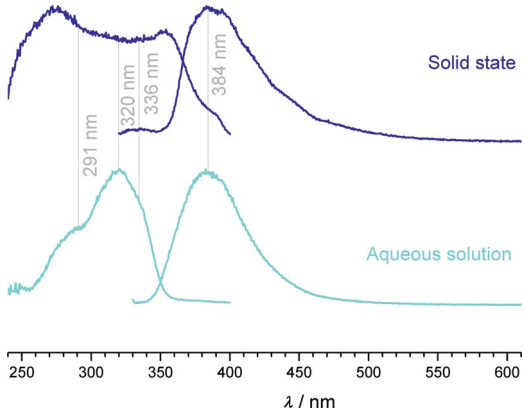

Figure 5. Excitation (λ_{em} = 420 nm) and emission [λ_{ex} = 275 nm (s)/320 nm (aq.)] spectra of CpOMe in the solid state (blue curve) and in Tris (0.1 M, pH 7.4) aqueous solution (cyan curve).

For the emission spectra, both solution and solid-state samples exhibit a maximum at 384 nm. Nevertheless, this emission goes up to 510 nm in solution and 560 nm in the solid state. The shape is then slightly different in the solid state compared to the smooth emission from solution. The quantum yield for this emission of CpOMe is around 38% (± 4%) upon excitation at 320 nm (maximum absorption) in solution and 31% (± 3%) in the solid state, so that no significant difference can be found here due to experimental error. It will be demonstrated below that these emission and

excitation spectra are retrieved in the DPApC ligand and in the lanthanide complexes together with additional emission and excitation components arising from the DPA backbone.

Luminescence of the DPApC Ligand and Its Europium Complex

Excitation and emission spectra of $[Eu(DPApC)_3]^{3-}$ 1×10^{-4} M in Tris (0.1 M pH 7.4) and the solid $Cs_3[Eu(DPApC)_3]$ powder were measured at room temperature and at 77 K (10% glycerol added to the aqueous solution). Considerable differences in the excitation spectra were observed between the aqueous solution and the solid state (Figure 6). First of all, the absorption bands of the direct f–f transition are observed. The most intense one is the $^5L_6$ (excitation at 395 nm); the $^5D_2$ at 464.5 nm is also rather strong, whereas the $^5D_3$ and $^5D_1$ are less intense. Then, the absorption band of the coumarin chromophore is also different in the solid state relative to that in aqueous solution. The absorption range is extended to the visible range up to the peak of the $^5L_6\leftarrow{}^7F_0$ and $^5D_3\leftarrow{}^7F_0$ transitions.

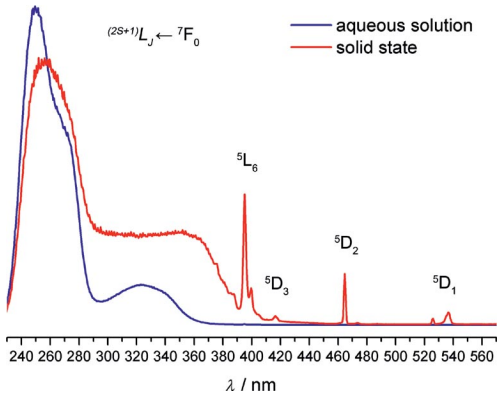

Figure 6. Excitation spectra of $[Eu(DPApC)_3]^{3-}$ aqueous solution (1×10^{-4} M in Tris 0.1 M, pH 7.4, blue curve) and $Cs_3[Eu(DPApC)_3]$ solid state sample (red curve), both at room temperature with λ_{em} = 615 nm.

Regarding the emission spectrum upon 320 nm excitation (Figure 7), the major difference between the solution and the solid state is provided by the emission of the coumarin. A significant bathochromic shift of the emission band of the coumarin is observed in the whole excitation range. The maximum is located at 389 nm in aqueous solution and 411 nm in the solid state. In addition, the $^5L_6\leftarrow{}^7F_0$ transition is also slightly visible in the emission spectrum in the solid state. This is due to the reabsorption of the coumarin emission by the europium ion (by a direct f–f transition, no energy transfer involved), thus reinforcing the emission of the sensitized europium. The bathochromic shift of the coumarin emission in the solid state may also be due to a reabsorption-linked phenomenon. Indeed, the excitation spectra of the solid-state sample have shown that absorption can go up to 400 nm, with strong absorption still occurring at 380 nm. Consequently, part of the emission of the coumarin that would take place below 380 nm can be significantly reabsorbed by the ligand. As the maximum of the emission is located near this region, reabsorption shifts it towards higher wavelengths.

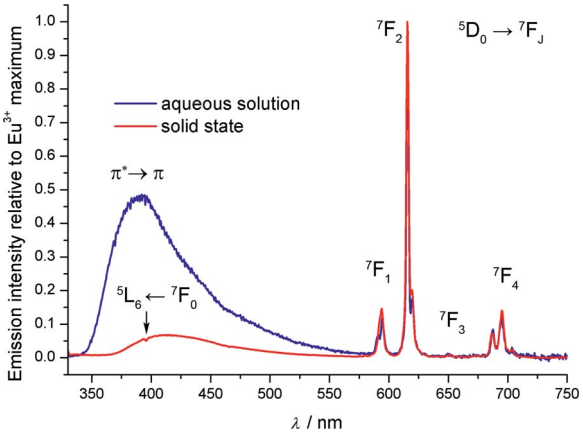

Figure 7. Emission spectra (λ_{ex} = 320 nm, room temperature) of aqueous solution of $[Eu(DPApC)_3]^{3-}$ (1×10^{-4} M in Tris 0.1 M, pH 7.4, blue curve) and solid-state sample of $Cs_3[Eu(DPApC)_3]$ (red curve) normalized by the maximum emission intensity from the Eu^{3+} ion ($^5D_0\rightarrow{}^7F_2$ transition).

As seen in Figure 7, the emission of the coumarin is also greatly decreased in the solid state, relative to the emission of europium. The maximum emission of the coumarin in aqueous solution is up to 50% of the $^5D_0\rightarrow{}^7F_2$ europium transition, while it is less than 10% in the solid state. The emission peaks from the coumarin and europium can be integrated (Table S1). Europium emission represents 48% of the total emission in the solid state, which means that coumarin and europium emit a similar amount of photons (the ratio of coumarin emission to europium emission is 1.1). In aqueous solution, europium emission represents only 12% of the total emission. The coumarin then emits 7.4 times more photons than europium. With respect to the europium emission, the only structural difference between the solid sate and the solution is due to the $^5D_0\rightarrow{}^7F_1$ transition, which is split in two in aqueous solution, consistently with the emission from tris(dipicolinato)europium.[13] This difference in relative intensity between europium and coumarin induces a significant shift in color. Under excitation with a long-wave UV lamp (366 nm), the solid state sample looks magenta, whereas in solution, the color has a stronger blue component and looks more lavender-colored. Upon excitation at 254 nm (short-wave UV lamp), the color becomes nearly as red as $Cs_3[Eu(dipic)_3]$, most of the blue component from coumarin being lost.

The excitation spectra with λ_{em} = 615.5 nm, either in the solid state or in aqueous solution, are different from the ones for the emission at 411 nm (solid) or 389 nm (aqueous solution). The ratio of the europium maximum emission peak ($^5D_0\rightarrow{}^7F_2$ transition, 615.5 nm) and to that of the coumarin (411 nm) was measured from the excitation spectra of the solid-state sample (Figure S7), and the results are presented in Figure S8. A fairly constant ratio is observed from 310 to 340 nm, where the absorption range of the coumarin chromophore is mainly located. Below 310 nm, the

absorption of the DPA moiety becomes significant in the solid samples, whereas at higher wavelengths, the additional absorptions, which probably come from intermolecular interactions as well as f–f transitions, are responsible for the europium emission. This also rationalizes the red color under the 254 nm UV lamp, as the ratio of coumarin to europium emission in Figure S8 falls down to 0.1 at 250 nm excitation.

To summarize, there are quite important differences in photophysical properties between powder solid state samples and those in solution. Many of these differences arise from the difference in molecular surroundings and induce modulations of both excitation and emission characteristics. The photophysical behavior in aqueous solution will now be deeply investigated and presented in order to better understand the mechanism, and thus the efficiency and shortcomings of such a molecular system for europium sensitization.

Sensitization Pathway

Ligand-Centered Photophysical Properties

The excitation and emission spectra of the free ligand DPApC, together with its gadolinium and europium complexes are presented in Figure 8. Excitation at 320 nm of $(DPApC)^{2-}$ or $[Gd(DPApC)_3]^{3-}$ results in a ligand-centered emission, displaying one broadband with a maximum around 26000 cm^{-1} (384 nm), which sustains a hypsochromic shift of about 15 nm upon decreasing the temperature at 77 K. At 77 K, a faint second band is observed, which becomes exclusive upon time resolution with a 50 μs delay. For the nonemissive Gd complex, this band is more intense and makes the room temperature spectrum look broader. Upon time resolution, the same spectrum as that of the free ligand is observed with a maximum at 490 nm [(0-phonon component at 463 nm, (21600 cm^{-1})], and it extends from 440 up to 630 nm, with a vibrational progression close to 1200 cm^{-1}, which is typical of Gd complexed with aromatic backbones. The high-energy band is thus attributed to a singlet state emission from the ligand, whereas the band at lower energy upon time resolution is attributed to a triplet state of the ligand. Compared to DPApR series,[18] the triplet of the DPApC ligand is redshifted by approximately 90 nm.

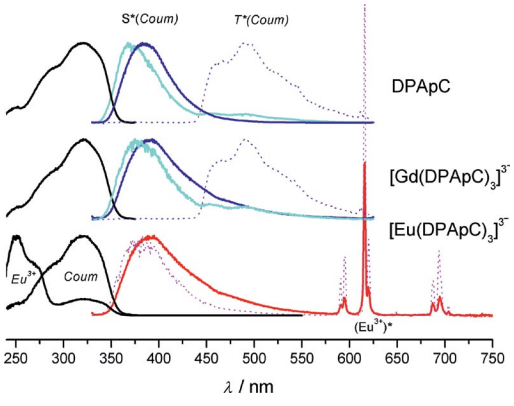

Figure 8. Excitation (black curves) and emission spectra (λ_{ex} = 320 nm) of the uncoordinated ligand as well as its gadolinium and europium complexes at room temperature (solid curves) and 77 K (solid cyan and dotted magenta curves). Emission from the ligand triplet state (dotted purple curves) recorded 50 μs after 320 nm excitation pulses. 1×10^{-4} M in Ln^{3+} ion, 3×10^{-4} M in ligand in Tris (0.1 M aqueous solution, pH 7.4) and 10% glycerol for frozen solutions.

Europium-Centered Photophysical Properties

In the presence of an emissive lanthanide, the characteristic metal-centered emission lines arising from the Eu^{3+} $^5D_0$ excited states are observed upon excitation at 280 nm or 320 nm. The broad band at 384 nm is, however, still present and accounts for about 88% of the Eu^{III} complex signal (total emission) at room temperature and 57% at 77 K. When the luminescence decays are sampled with short time intervals, the function is monoexponential, reflecting lifetimes for the Eu^{3+} $^5D_0$ excited states of 1.4 ± 0.1 ms at room temperature and 2.2 ± 0.1 ms at 77 K. These values are comparable to those recorded within the DPApR series. The temperature dependence of the lifetimes reflects the presence of some vibrational quenching processes of the Eu excited state by the ligand backbone, as already observed with DPApR series.[18] Quantum yields for these emissions at room temperature were measured in an integration sphere.[41] Lifetimes and emission spectra were then used to calculate the radiative lifetime as well as the intrinsic quantum yield and sensitization efficiency of the europium emission, according to Equations (5) to (7) in the Experimental Section. The results are presented in Table 1.

Table 1. Quantum yields, Φ_L^{L+Ln}, of the ligand and lanthanide emission upon ligand excitation, Φ_L^{L}, of the ligand residual emission; intrinsic quantum yields, Φ_{Ln}^{Ln}, of the lanthanide ion upon lanthanide excitation; observed lifetimes, τ_{obs}^{Ln}, of the lanthanide emission and radiative lifetimes, τ_r^{Ln}, of the lanthanide ion; sensitization efficiency, η_{sens}, of the ligand and its gadolinium and europium complexes in Tris (0.1 M, pH 7.4) in aqueous solution except for entry marked with [a] (solid-state powder). Error in τ_{obs}: ± 0.1 ms; 10% relative error in the other values; λ_{ex} = 320 nm.

	$[Eu(DPApC)_3]^{3-}$	$Cs_3[Eu(DPApC)_3]$[a]	$[Gd(DPApC)_3]^{3-}$	DPApC
Φ_L^{L+Ln}	0.113	0.141	0.115	–
Φ_L^{L}	0.097	0.093	0.115	0.316
Φ_{Ln}^{Ln}	0.016	0.048	0	–
τ_{obs}^{Ln} /ms	1.4, 2.2[b]	1.4	0	–
τ_r^{Ln} /ms	4.2	2.8	0	–
Φ_{Ln}^{Ln}	0.33	0.50	0	–
η_{sens}	0.048	0.097	0	–

[a] Solid state powder; refractive index n = 1.517. [b] 77 K.

Interestingly, the emission quantum yield of the uncoordinated ligand is much higher than either its gadolinium or its europium complex, 31.6% of the absorbed photon being reemitted in aqueous solution. The gadolinium complex reemits only 11.5% of the absorbed photons and the europium complex 11.3%, whereas 9.7% of the absorbed photons are emitted by the coumarin moiety and only 1.6% by

the europium ion. These decreases in quantum yield upon lanthanide coordination can be accounted either by structural changes of the ligand upon complexation, affecting its photophysical properties, or by the influence of the coordinating ion on the photophysical properties, such as on the relaxation of the forbidden triplet state formation (intersystem crossing, ISC). Indeed, the highly paramagnetic gadolinium ions induce a higher ISC rate and hence increase the population of the triplet state.[42,43] Nevertheless, as triplet states are by essence long-lived, quenching of the triplet states can be a quite effective way of nonradiative deactivation. Most of the energy stored in the triplet state would then be lost by nonradiative deactivation, and hence, the overall quantum yield for the mixed emission from singlet (fluorescence) and triplet (phosphorescence) states would be decreased as a result of the decrease in fluorescence quantum yield that is related to the increase in the ISC rate.

For $[Eu(DPApC)_3]^{3-}$, part of the triplet state energy is transferred onto the europium ion and gives rise to the observed characteristic europium emission. The percentage of each component responsible for the total emission was estimated from the integration ratio of each part of the emission spectrum and amounts to 58.8% for the singlet emission, 27.0% for the triplet emission, and 14.2% for the europium emission, at room temperature. The phosphorescence was extracted by subtracting the normalized emission spectrum of the uncoordinated ligand, which shows very little or no phosphorescence at room temperature, from the normalized emission of the europium complex. The normalization was done with respect to the maximum of the coumarin emission at 389 nm. Most of the emission arises from the singlet state with more than half of the intensity emitted as fluorescence. Nevertheless, a significant contribution to the emission from the triplet state is observed (27%), certainly accounting for the important thermally assisted back-transfer from the excited europium ion to the ligand triplet state. Finally, a fair 14.2% comes from the europium ion. These results then suggest that the low quantum yield of the europium emission comes from a low net energy transfer rate due to significant back-transfer.

Compared to the $[Eu(dipic)_3]^{3-}$ complex, the dipic complex has a higher quantum yield (Φ_{dipic}^{Eu} = 24% vs. Φ_{DPApC}^{Eu} = 1.6%). Nevertheless, two important factors are to be taken into account. First, the excitation of the dipic complex can only take place below 300 nm, and second, its extinction coefficient is also smaller with an $\varepsilon_{270}([Eu(dipic)_3]^{3-})$ of 16470 $1mol^{-1}cm^{-1}$ at 270 nm vs. $\varepsilon_{320}([Eu(DPApC)_3]^{3-})$ = 25286 $1mol^{-1}cm^{-1}$ at 320 nm. As a consequence, $\Phi_{dipic}^{Eu}/\Phi_{DPApC}^{Eu}$ = 15, while the $\varepsilon\Phi_L^{Eu}$ ratio is only a factor of 10, which makes DPApC an interesting candidate, considering the gain of 50 nm in excitation wavelength.

As observed from Figure 9, the difference in europium intensity between room temperature and low temperature depends on the excitation wavelength. The difference in emission intensity is maximal upon excitation around 320 nm, whereas it is much weaker upon excitation at 280 nm. The excitation of the coumarin at 320 nm and the resulting transfer to the europium ion is then much more temperature-dependent than the excitation at 280 nm, where most of the excitation is on the DPA moiety.

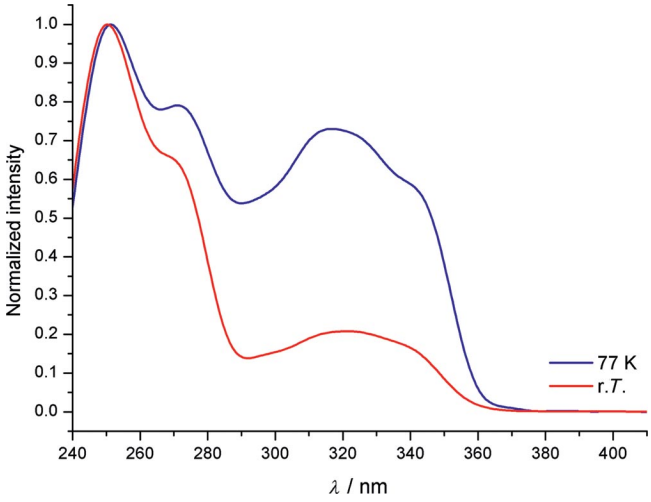

Figure 9. Smoothed (FFT filter, 5% cutoff) normalized excitation spectra for the emission of the $^5D_0 \rightarrow {}^7F_2$ europium transition at room temperature (r.t.) and at low temperature (77 K).

To better understand the sensitization pathway, low-temperature, time-resolved measurements were carried out on the uncoordinated ligand and its gadolinium complex, with excitations at 320 and 270 nm (Figure 10). At 77 K, a second phosphorescence band centered at 410 nm appears upon excitation at 270 nm, which is not observed upon excitation at 320 nm. As a comparison, the scaled phosphorescence spectrum of the dipicolinate gadolinium complex $[Gd(dipic)_3]^{3-}$ is also shown in Figure 10 (green line): its triplet emission is located at the exact position of the higher-energy triplet emission. This could indicate that this new band comes from the DPA moiety of the DPApC ligand, whereas the other triplet emission that is visible upon both excitations arises from the coumarin moiety. However, the same phenomenon was also observed when measuring the polyoxyethylene coumarin chromophore CpOMe (Figure 11), meaning that the high energy triplet emission can, in fact, come from either the coumarin moiety or the coordinating DPA.

The most rational explanation would be that two triplet excited states can be populated on the coumarin chromophore, depending on the excitation wavelength. The one higher in energy can be reached by an excitation at 270 nm and is located at the same energy as the DPA triplet state. The second one is reached at 320 nm, where no excitation of the DPA moiety can take place. Its energy is lower than the one excited at 270 nm, but can also be populated upon excitation at 270 nm. This is perfectly coherent, because of the internal conversion from higher excited state to lower excited state.

To confirm this hypothesis, calculations of the molecular orbitals with INDO/S parameters after optimizing the geometry with ZINDO INDO/1 calculations were performed with the Scigress Explorer software.[44] Two absorption

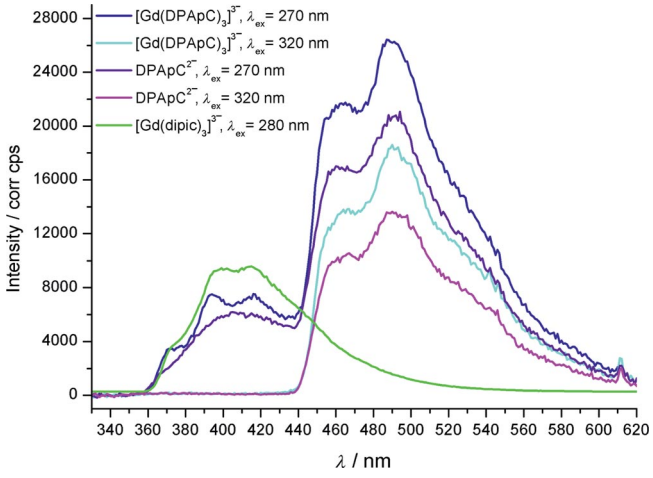

Figure 10. Triplet emission of the DPApC ligand and its gadolinium complex 50 μs after pulsed excitation. $[DPApC^{2-}] = 3 \times 10^{-4}$ M, $[Gd^{3+}] = 1 \times 10^{-4}$ M in a frozen Tris 0.1 M aqueous solution (10% glycerol), pH 7.4, $T = 77$ K. Emission of $[Gd(dipic)_3]^{3-}$ scaled to show location of the triplet emission.

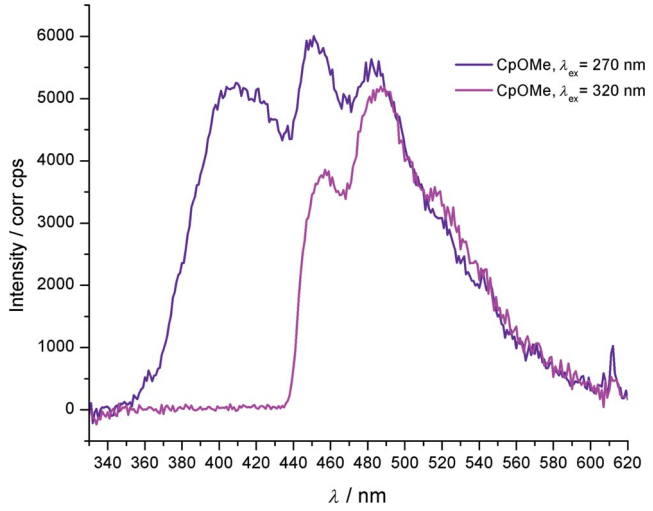

Figure 11. Triplet emission of the polyoxyethylene coumarin chromophore (CpOMe) 50 μs after pulsed excitation. Frozen saturated solution diluted 10× in Tris (0.1 M aqueous solution containing 10% glycerol, pH 7.4) at $T = 77$ K.

bands at 286.5 nm and at 309.9 nm were predicted and attributed to π–π* transitions (Supporting Information, Figure S9). The band located at 309.9 nm is more intense than the one at 286.5 nm. It involves the same π HOMO as the band at 286.5 nm, but lower π_α* LUMO, relative to the higher energy π_β* molecular orbital. Finally, a third weak transition is predicted at 348.6 nm and is attributed to an n–π* transition from an n HOMO to the π_α* LUMO. The n–π* transition is very weak in accord with its forbidden character and is barely seen in the experimental UV/Vis absorption or excitation spectrum (Figure S5) as a slight shoulder at 340 nm. The most intense π–π_α* transition is experimentally observed as the absorption maximum at 320 nm, whereas the more energetic π–π_β* transition is observed in the excitation spectrum as an apparent shoulder at 284 nm. Similar calculations performed on the DPApOMe ligand demonstrated that one major π–π* transition (predicted at 272.5 nm) is responsible for the absorption around 270 nm (Supporting Information, Figure S10).

The wavelength-dependent difference between low-temperature and room-temperature excitation spectra can then be rationalized according to Figure 12.

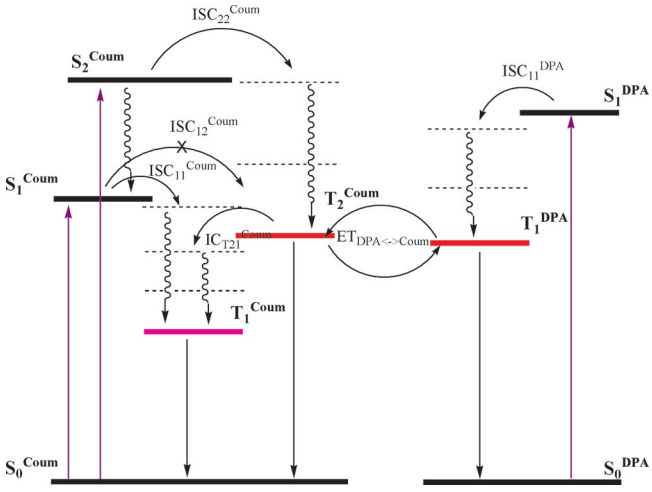

Figure 12. Relative energy diagram of the coumarin (Coum) and dipicolinate (DPA) moieties with their possible interactions (ISC_{xy}: Intersystem crossing from the xth to the yth excited state, $ET_{L<->C}$: Energy transfer between ligand L and chromophore C, IC_{Txy}: internal conversion from the xth triplet excited state to the yth triplet excited state). Wavelet arrows point at nonradiative deactivation, whereas straight arrows point at radiative transitions (absorptions: solid purple, emissions: solid black). Thick black lines indicate the lower energy states of the singlet ground (S_0) or nth excited states (S_n), thick colored lines indicate the lower energy states of the triplet nth excited states (T_n) and dashed black lines are higher vibrational modes of the parent lower energy states.

Single pathway $T_1^{Coum} \rightarrow$Eu: Upon 320 nm excitation, the absorption by the coumarin moiety promotes an electron from the π HOMO to the π_α* LUMO of the chromophore, followed by an ISC from this singlet $^1\pi\pi_\alpha$* excited state (1st excited state of the coumarin, S_1^{Coum}) to its triplet state $^3\pi\pi_\alpha$* (T_1^{Coum}). Then, an energy transfer (ET) to the europium ion can occur, as this triplet state ($^3\pi\pi_\alpha$*) is located above the emissive $^5D_0$ spectroscopic level of the europium ion. Nevertheless, due to the relative proximity of the $^3\pi\pi_\alpha$* excited state of the ligand with the accessible europium spectroscopic levels, a non-negligible back-transfer from the europium excited level to the $^3\pi\pi_\alpha$* state of the ligand also occurs.

Mixed pathway $\{T_2^{Coum} \leftrightarrows T_1^{DPA}\} \rightarrow$Eu: When the excitation wavelength is at higher energy, such as 270 nm, the absorption on the coumarin promotes an electron to another molecular orbital, the π_β*, higher in energy than the π_α* LUMO. After ISC from the singlet $^1\pi\pi_\beta$* (2nd excited state of the coumarin, S_2^{Coum}) to the triplet $^3\pi\pi_\beta$* (T_2^{Coum}), the triplet can undergo an internal conversion to the lower $^3\pi\pi_\alpha$*, in which case the same problem is encountered as

upon 320 nm excitation. Alternatively, it can directly transfer its energy to the europium ion, with little issues of back-transfer now, or transfer its energy to the DPA moiety (which has a triplet excited state located in the same region of the spectrum). The transfer to the DPA $^3\pi\pi^*$ state would then offer another pathway to efficiently sensitize the europium ion with very little or no back-transfer to the original ligand triplet state. Finally, absorption of the 270 nm excitation light source can also directly promote an electron from a π MO of DPA moiety to a π* ($^1\pi\pi^*$ state or S_1^{DPA}), which, after ISC, becomes a $^3\pi\pi^*$ system (T_1^{DPA}) with energy similar to the $^3\pi\pi_\beta^*$ state and offers the same alternatives to the $^3\pi\pi^*$ relative to the $^3\pi\pi_\beta^*$.

Nevertheless, the $^3\pi\pi_\alpha^*$ state remains accessible wherever the sensitization comes from. Thus, back-transfer should be independent of the sensitization pathway. On the other hand, what ought not to be the same is the energy transfer rate from either a $^3\pi\pi_\beta^*$ or a $^3\pi\pi_\alpha^*$. It then becomes obvious that the higher triplet state ($^3\pi\pi_\beta^*$) has a higher energy transfer rate to the europium ion than the LUMO so that the global transfer rate taking into account the unavoidable back-transfer to the $^3\pi\pi_\beta^*$ is increased upon 270 nm excitation.

Luminescence of the Europium Complex in Different Solvents

Emission of coumarins is known to be dependent on the solvent in which they are dissolved. Yet, it has been shown that 7-hydroxy-based coumarins are less apt to strong solvatochromism than 7-amino-based coumarins. This behavior is rationalized by taking into account the different deactivation pathways of the excited state that these two types of fluorophores experience.[38] In order to check the influence of the coumarin in our system, its photophysical properties were measured in different solvents. EtOH, DMSO, and Tris-buffered H_2O were tested as pure solvents or as mixtures.

Table 2 shows the quantum yields, lifetimes, and sensitization efficiencies for the emission of $[Eu(DPApC)_3]^{3-}$ in Tris-buffered water (pH 7.4), ethanol, or DMSO. Similar quantum yields for the europium emission upon excitation at 320 nm were measured in water and ethanol (ca. 1.5%), while the value decreases drastically in DMSO (ca. 0.2%). The emission of the coumarin part is more affected by the solvent, with $\Phi_L^L \approx 11\%$ in water, ca. 13% in ethanol, and only ca. 5% in DMSO. However, lifetimes of the Eu^{3+} $^5D_0$ excited state follow the opposite trend, ranging from τ = 1.45 ms in water to 2.11 ms in DMSO. Sensitization efficiencies of ca. 4% were calculated in water and ethanol but only 0.4% in DMSO. This low efficiency explains the lower overall quantum yield in DMSO despite a higher intrinsic quantum yield (53%). Furthermore, as the coumarin emission is also lower in DMSO than in the other two solvents, it seems that DMSO is a good quencher of the ligand excited states, but not of the europium.

Table 2. Quantum yields, lifetimes, and sensitization efficiencies of a 1×10^{-4} M solution of $[Eu(DPApC)_3]^{3-}$ in different solvents. Error in τ : ± 0.05 ms; 10% relative error in the other values; λ_{ex} = 320 nm.

	H_2O Tris 0.1 M[a]	EtOH[b]	DMSO[c]
Φ_L^{L+Eu}	0.120	0.142	0.051
Φ_L^{L}	0.106	0.127	0.049
Φ_L^{Eu}	0.014	0.015	0.002
τ_{obs}^{Eu} /ms	1.45	1.85	2.11
τ_r^{Eu} /ms	4.6	4.6	4.0
Φ_{Eu}^{Eu}	0.32	0.40	0.53
η_{sens}	0.044	0.037	0.004

[a] n = 1.333. [b] n = 1.361. [c] n = 1.4785.

Mixtures of two solvents were also investigated. Figure 13 presents the ratio of coumarin to europium emission, and Figure S11 (Supporting Information) shows the quantum yields for the europium and coumarin emission. When increasing the ethanol percentage in a water solution, the quantum yield is maximal at 20% of ethanol, then falls down and is again increased in pure ethanol. The coumarin emission is maximal with 40% of ethanol and then keeps gently decreasing up to 100% ethanol. When it comes to the ratio of coumarin to europium emission, we observe a maximum with 60% ethanol. In a mixture of water/DMSO, the quantum yield is maximal for 20% of DMSO and decreases in pure DMSO, whereas the coumarin emission is maximal at 40% DMSO. Interestingly, the ratio keeps increasing with increasing percentage of DMSO, so that it might be used to determine the ratio of DMSO in Tris-buffered water. This can be of interest for analytical applications, to determine the amount of DMSO present in water solutions.

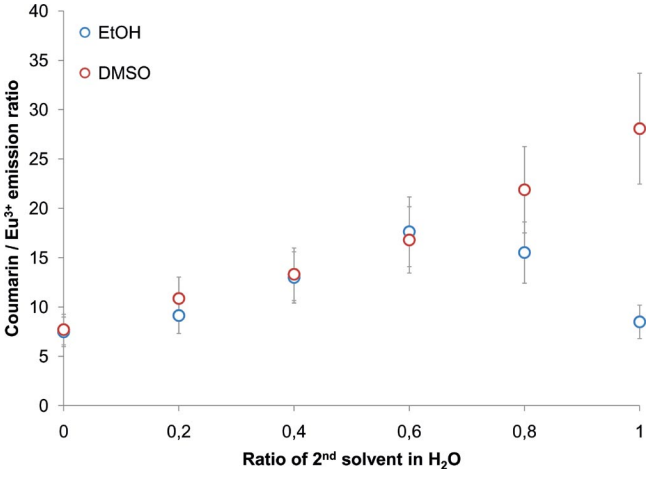

Figure 13. Ratio of the coumarin to europium emission as a function of solvent mixture (1×10^{-4} M in complex, λ_{ex} = 320 nm).

Europium Complex with Mixed Ligands

According to the literature, the coordination ability of the dipicolinate moiety (DPA) in DPApR ligands is slightly affected by the nature of the R group.[18] Hence, we can

obtain mixed Eu/dipic/DPApC complexes by mixing both ligands in different ratios in the range $0.33{:}x{:}(3-x)$ with x = 0–3. In the following discussion, the $[Eu(dipic)_x(DPApC)_{3-x}]$ complexes will be labeled as $[x{:}(3-x)]$ for purposes of clarity.

The quantum yield upon excitation at 280 nm is maximum with the $[Eu(dipic)_3]^{3-}$ complex [3:0] and is decreased when a lower ratio of dipic ligand is in solution (Figure 14). The $[Eu(DPApC)_3]^{3-}$ complex [0:3] has the lowest quantum yield of this series, whereas the mixed-ligand complexes have intermediate values. On the other hand, absorption increases from the [3:0] to [0:3] complex; the DPApC ligand is a better absorber than the dipic one.

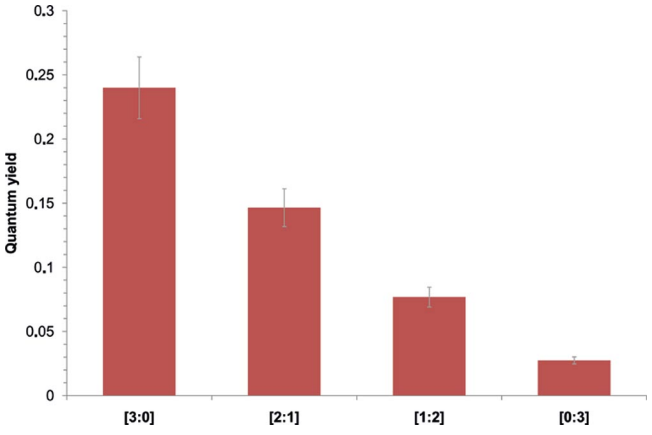

Figure 14. Quantum yields of the pure and mixed-ligand complexes upon excitation at 280 nm, Tris (0.1 M aqueous solution, pH 7.4), 1×10^{-4} M in complex.

When it comes to the excitation at 320 nm (Figure S12), the trend is the opposite. The [3:0] complex cannot be excited at this wavelength in solution. However, as soon as a DPApC ligand is introduced, excitation can take place and gives rise to a europium emission. The gain in europium intensity between [0:3] and the mixed-ligand [1:2] and [2:1] complex is here less important than the decrease in intensity with excitation at 280 nm. More than 75% of the emission intensity of the pure complex (the most emissive of the series) is conserved with only one equivalent of sensitizing ligand, only 40% remains upon excitation at 280 nm with one equivalent of the dipic ligand. There are several explanations to this different loss in intensity. First of all, when the number of dipic ligands is decreased, the probability that they absorb the incoming light is reduced. Then, fewer photons will be absorbed by the dipic ligand and transferred to the europium center with the high sensitization efficiency of this ligand. Second, and according to the location of the triplet state of each kind of ligand, a nonradiative transfer from the excited dipic ligand to an unexcited DPApC ligand might occur and hence further decrease the amount of net sensitization of the europium. The third point is that, the europium, once sensitized, can back-transfer its excitation to the DPApC ligand, as observed in the present work. As soon as a DPApC ligand is coordinated, back-transfer should become more relevant.

To further prove this assumption, lifetime measurements were conducted at room temperature. The higher lifetime was found for the $[Eu(dipic)_3]^{3-}$ complex [1.55(5) ms], and the lifetime slightly decreased in [2:1] [1.49(5) ms], [1:2] [1.44(5) ms], and $[Eu(DPApC)_3]^{3-}$ [1.42(5) ms]. Even if the observed lifetimes are not significantly different, a general lowering trend can be reasonably deduced despite the experimental error, at least between 1.55(5) and 1.42(5) ms. As the observed lifetime is a good indicator of the quenching of the europium excited state, the affirmation that more back-transfer is introduced as the ratio of DPApC is increased relative to the dipic ligand is consistent both with the experimental data and the sensitization hypothesis.

Quantum yields upon excitation at 320 nm were then measured for the europium and coumarin emissions. As shown in Figure 15, both europium and coumarin quantum yields increase when changing the stoichiometry from the pure $[Eu(DPApC)_3]^{3-}$ to increasing amounts of dipic ligand. Nevertheless, absorption at 320 nm is of course reduced when the complex concentration is kept constant until no more photons are absorbed at 320 nm by the pure $[Eu(dipic)_3]^{3-}$ complex. The inverse of these quantum yields were then plotted as a function of DPApC concentration. The fit showed a good linearity, thus confirming a Stern–Volmer deactivation kinetics, according to Equations (1) to (4) in the Experimental Section.

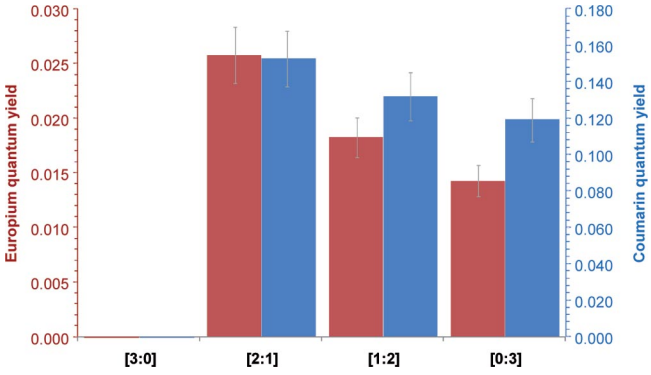

Figure 15. Quantum yield for the europium (red) and coumarin (blue) emission of the mixed-ligand complexes upon excitation at 320 nm.

Stern–Volmer plots for the emission of europium and coumarin as a function of [DPApC] (Supporting Information, Figure S13) point to a self-quenching of the coumarin excited states by the coumarin moiety itself. From the linear fits of both emissions, the emission quantum yields without quenching can be extracted as the inverse of the y-intercepts. Thus, $\Phi_{em}{}^0(Eu^{3+})$ = 4.3%, whereas $\Phi_{em}{}^0(Coum)$ = 17.7%. This means that the emission of the coumarin is quenched by 40% by the coumarin moiety itself in the pure $[Eu(DPApC)_3]^{3-}$ complex and that nearly 70% of the europium emission is also quenched by the coumarin, probably by energy back-transfer to its low-lying triplet excited state.

By use of the radiative lifetime of europium found in Table 1 and approximation of the radiative lifetime of the coumarin emission in the nanosecond range, we found that

the quenching rate for the europium emission is near a diffusion-limited quenching rate according to the Stokes–Einstein relation. On the other hand, the coumarin emission is quickly quenched, much quicker than the diffusion rate, since quenching should happen in the picosecond range.

In order to further check this behavior, solutions with 0.33 and 0.66 equiv. DPApC ligands and hence 2.66 and 2.33 equiv. dipic ligands, respectively, were prepared. The resulting emission of the coumarin was found to follow the Stern–Volmer plot, whereas the emission of the europium was too weak to be properly integrated (Figure S13). The advantage of mixing dipic and DPApC ligands is that the DPApC can be diluted without diluting the Eu^{3+}, thus really changing the ratio of DPApC/Eu^{3+}. Furthermore, since the dipic ligand does not absorb at 320 nm, no photophysical interactions should occur. The constant Eu/Ligand^{tot} ratio being set at 1:3, a constant concentration of the complex is kept, so that only the effect of the dilution of the coumarin sensitizing group can be studied in this way.

Conclusions

A photophysical study of *para*-polyoxyethylene dipicolinic acid derivatives coupled to methylumbelliferone as ligand for europium complex is reported. This new class of ligands is easily synthesized and its coordination to a europium ion gives the desired 1:3 complex under stoichiometric conditions, with properties quite similar to those already obtained with tris(dipicolinato) complex in terms of stability and coordination environment. The complex can be excited at 280 nm, corresponding to the DPA backbone of the ligand, but, additionally, due to the presence of the coumarin chromophore, the excitation range is expanded up to 360 nm in aqueous solutions and up to 400 nm in the solid state. This opens perspectives in view of exciting the dipicolinato complexes at a higher wavelength than in the shortwave UV. Reaching excitation wavelengths in the near-visible range can give access to applications in several domains, such as biology, color reproduction, or document security. The coumarin chromophore can be introduced in the ligand, but other dipicolinato complexes can also be doped with a few percent of the DPApC ligand, as stated above. As a drawback, a significant thermally assisted back-transfer from the excited europium ion to the lowest triplet state of the ligand was highlighted. A careful investigation of the triplet excited sates of the ligand together with the ones of the uncoupled moieties by time resolved emission spectrometry showed that the coumarin moiety possesses two excited states coming from π–π* transitions to two different π* molecular orbitals. A difference in energy transfer from these triplet states may explain the difference in europium quantum yields upon excitation at low energy (320 nm, Φ_L^{Eu} = 1.4%) or higher energy (270 nm, Φ_L^{Eu} = 2.7%). An increase in energy transfer from the higher triplet state is then needed in order to rationalize the higher emission quantum yield upon 270 nm excitation, since back-transfer to the lowest triplet state ought to be independent of the sensitization pathway. This complex has also shown potential in analytical applications due to the sensitivity of the coumarin emission to the solvent. Binary mixtures of DMSO with Tris-buffered water was found to be particularly well suited for this complex, since emissions of the europium and coumarin are differently affected by the increase in DMSO content. This gives access to a method of determining the content of DMSO in a water solution. Finally, complexes with two ligands, DPApC and dipic, were prepared at different ratios of ligands. This study revealed that the quantum yield for either the coumarin emission or the europium emission is self-quenched by the DPApC ligand upon excitation of the coumarin moiety at 320 nm. This technique offers a new tool in the rationalization of the europium sensitization by considering the self-quenching of the ligand as a possible factor of deactivation.

To conclude, the advantage of this class of ligand over many other ligands is that: first, it allows to finely tune the sensitization efficiency and extinction coefficient by a careful choice of the coupled chromophore, without significantly interfering with the coordinating ability of the dipicolinate moiety as long as the chromophore is noncoordinating; second, it offers a huge scope of derivatization with potential abilities in biological media; and finally, it provides a unique framework for the investigation and better understanding of the photophysical properties of luminescent lanthanide complexes.

Experimental Section

General Procedures: Solvents were purified by a nonhazardous procedure by passing them through activated alumina columns (Innovative Technology Inc. system).[45] Chemicals were ordered from Fluka and Aldrich and used without further purification. ESI-MS spectra were obtained with a Finningan SSQ 710C spectrometer by using 10^{-5}–10^{-4} M solutions in acetonitrile/H_2O/acetic acid (50:50:1) or MeOH, a capillary temperature of 200 °C, and an acceleration potential equal to 4.5 keV. The instrument was calibrated with horse myoglobin standard and analyses were conducted in the positive mode with a 4.6 keV ion spray voltage. Mass spectrometry experiments were performed by Dr Laure Ménin and elemental analyses by Dr. E. Solari, at the École Polytechnique Fédérale de Lausanne. ^{1}H NMR spectroscopy was performed with a Bruker Avance DRX 400 spectrometer and ^{13}C NMR spectroscopy with a Bruker AV 600 MHz instrument at 25 °C, with deuteriated solvents as internal standards. Chemical shifts are given in ppm relative to TMS.

Physicochemical Measurements

Spectrophotometric Measurements

Analytical grade solvents and chemicals were used without further purification. Aqueous solutions were prepared from doubly distilled water. Lanthanide solutions were prepared from the corresponding perchlorate salt and titrated by complexometry with a standardized Na_2H_2EDTA solution in urotropine-buffered medium and with xylenol orange as indicator.[46]

UV/Vis absorption spectra were measured with a Perkin–Elmer Lambda 900 spectrophotometer by using 1 cm path length quartz cells. Factor analysis and mathematical treatment of the spectrophotometric data were performed with the SPECFIT program.[47]

Luminescence Measurements

Luminescence measurements were recorded with a Fluorolog 3–22 spectrofluorometer from Jobin–Yvon. Emission and excitation spectra were measured in 1 cm path length quartz cells or quartz Suprasil® capillaries at room temperature and in quartz Suprasil® capillaries at 77 K with 10% glycerol added to the solutions. Room temperature measurements in quartz Suprasil® capillaries were performed in an integration sphere.[41] All emission spectra were measured in photon counts and corrected for the instrumental function. Luminescence evolution of the europium complex was performed by variation of the pH in a fashion similar to that in the titration of the ligands but on a 1:3 europium/ligand solution.

Quantum yields were determined in the integration sphere by measuring the ratio of the emitted corrected intensity to the absorbed corrected intensity.[41] Empty capillaries were used as blank. The obtained values were checked by comparison to the tris(dipicolinato)europium standard, which exhibits 24% quantum yield in Tris-buffered aqueous solutions at pH 7.4.[11] In solution, all concentrations were set at 1×10^{-4} M, including the concentration of the reference tris(dipicolinato) complex. For solid-state samples, the complex or the uncoupled chromophore (CpOMe) was used as a powder.

Stern–Volmer plots were fitted by using Equations (1), (2), (3), and (4), where Φ_{em} is the emission quantum yield, Φ_{em}^0 is the emission quantum yield without quenching, k_q is the quenching rate, τ_{obs}^0 is the observed lifetime without quenching, [Q] is the concentration of quencher Q, k_r is the radiative emission rate ($k_r = 1/\tau_r$), and k_{obs}^0 is the sum of all deactivation rates for the excited state of the emissive molecule ($k_{obs}^0 = 1/\tau_{obs}^0$).

$$\frac{\Phi_{em}^0}{\Phi_{em}} = 1 + k_q \tau_{obs}^0 [Q] \quad (1)$$

$$\frac{1}{\Phi_{em}} = \frac{1}{\Phi_{em}^0} + k_q \frac{\tau_{obs}^0}{\Phi_{em}^0} [Q] \quad (2)$$

$$\Phi_{em}^0 = \frac{k_r}{k_{obs}^0} = \frac{\tau_{obs}^0}{\tau_r} \quad (3)$$

$$\frac{1}{\Phi_{em}} = \frac{1}{\Phi_{em}^0} + k_q \tau_r [Q] \quad (4)$$

Radiative lifetimes, τ_{obs}, intrinsic quantum yields, Φ_{Ln}^{Ln}, and sensitization efficiency, η_{sens}, were calculated according to Equations (5), (6), and (7).

$$\frac{1}{\tau_r} = k_r = A_{MD,0} n^3 (I_{tot}/I_{MD}) \quad (5)$$

$$\Phi_{Ln}^{Ln} = \frac{\tau_{obs}}{\tau_r} \quad (6)$$

$$\Phi_L^{Ln} = \eta_{sens} \Phi_{Ln}^{Ln} \quad (7)$$

In these equations, k_r is the radiative deexcitation rate, τ_{obs} is the observed lifetime upon radiative and nonradiative deactivation, $A_{MD,0}$ is the spontaneous emission probability for the purely magnetic dipole (MD) transition, whose intensity is practically not influenced by the chemical environment of the lanthanide ion ($^5D_0 \rightarrow {}^7F_1$ in Eu^{3+}, $A_{MD,0} = 14.65\ s^{-1}$), n is the refractive index of the solvent, and I_{tot}/I_{MD} is the ratio of total emission intensity to the emission intensity of the MD transition.[48]

Water molecules in the first coordination sphere were estimated by the Supkowski and Horrocks formulas [Equations (8) and (9)].

$$q = A[\tau_{obs}^{-1}(H_2O) - \tau_{obs}^{-1}(D_2O) - k_{XH}] \quad (8)$$

$$k_{XH} = \alpha + \beta n_{OH} + \gamma n_{NH} + \delta n_{O=CNH} \quad (9)$$

Here $\tau_{obs}(H_2O)$ is the lifetime in water, $\tau_{obs}(D_2O)$ is the lifetime in deuteriated water, and n_{XH} is the number of XH oscillators in the first coordination sphere.[39]

Synthesis of the Ligand: The synthesis of $Br(CH_2CH_2O)_3OMe$ (**2**) has already been reported in the literature, starting from 2-[2-(2-methoxyethoxy)ethoxy]ethanol and PBr_3, with yields of 18–25%,[49] whereas diethyl ester **4** was prepared from chelidamic acid.[18]

7-(Methylpolyoxyethylenyl)methylumbelliferone (CpOMe): To a solution of 7-hydroxy-4-methylcoumarin (**1**) (4.2 mmol, 0.74 g) in DMF (15 mL) was added K_2CO_3 (91.8 mmol, 12.7 g). The solution was stirred for 5 min and turned yellow. Compound **2** (4.2 mmol, 0.95 g) was then added dropwise, and the solution was stirred for 4 h at room temperature. Afterwards, the solvent was evaporated under reduced pressure, and the crude product was redissolved in CH_2Cl_2 (150 mL). The solution was washed three times with a saturated NH_4Cl solution (3×80 mL), dried with Na_2SO_4, filtered, and concentrated under reduced pressure to yield CpOMe (0.9 g, 66%). ^1H NMR ($CDCl_3$, 400 MHz): δ = 7.48 (d, J = 8.8 Hz, 1 H, H_{ar}), 6.88 (dd, J_1 = 8.8, J_2 = 2.5 Hz, 1 H, H_{ar}), 6.82 (d, J = 2.5 Hz, 1 H, H_{ar}), 6.13 (d, J = 1.1 Hz, 1 H, H_{ar}), 4.18 (m, 2 H, -CH_2-), 3.89 (m, 2 H, -CH_2-), 3.74 (m, 2 H, -CH_2-), 3.67 (m, 4 H, -CH_2-), 3.55 (m, 2 H, -CH_2-), 3.37 (s, 3 H, -CH_3), 2.39 (d, J = 1.1 Hz, 3 H, -CH_3) ppm.

7-(Hydroxypolyoxyethylenyl)methylumbelliferone (3): CpOMe (2.34 mmol, 0.75 g) was dissolved in CH_3CN (15 mL) under nitrogen. The solution was heated up to 60 °C and TMSI (3.51 mmol, 0.5 mL) was then added dropwise. The reaction mixture was stirred for 80 min at 60 °C before the solvent was evaporated under reduced pressure. CH_2Cl_2 (50 mL) was added to the remaining medium, and the solution was washed with an aqueous solution of $Na_2S_2O_3$(0.09 M, 50 mL). The brown aqueous solution was then extracted three times with CH_2Cl_2 (3×50 mL), and the collected organic solutions were dried with Na_2SO_4, filtered, and concentrated under reduced pressure to yield **3** (0.60 g, 80%). ^1H NMR ($CDCl_3$, 400 MHz): δ = 7.49 (d, J = 8.8 Hz, 1 H, H_{ar}), 6.89 (m, 1 H, H_{ar}), 6.84 (dd, J_1 = 2.4, J_2 = 1.2 Hz, 1 H, H_{ar}), 6.13 (d, J = 1.0 Hz, 1 H, H_{ar}), 4.19 (m, 2 H, -CH_2-), 3.90 (m, 2 H, -CH_2-), 3.73 (m, 6 H, -CH_2-), 3.62 (m, 2 H, -CH_2-), 2.39 (d, J = 1.0 Hz, 3 H, -CH_3) ppm.

Diethyl 4-[(4-Methylcoumarin-7-yl)oxypolyoxyethylenyl]dipicolinate (5): Compounds **3** (1.86 mmol, 0.60 g), **4** (0.93 mmol, 0.22 g), and PPh_3 (1.86 mmol, 0.49 g) were added into THF (15 mL). After dropwise addition of diisopropyl azodicarboxylate (DIAD) (1.86, 0.37 mL) to the solution, it was heated under reflux for three hours (controlled by TLC, CH_2Cl_2/MeOH, 97:3). The solvent was then evaporated under reduced pressure, and the remaining mixture was dissolved in CH_2Cl_2 (100 mL). The solution was washed three times with water (3×100 mL), dried with Na_2SO_4, filtered, and

concentrated under reduced pressure to yield 1.73 g of crude product, which was dissolved in a minimum amount of AcOEt and kept in a freezer overnight to yield a precipitate, which was filtered off. The precipitation was repeated until no solid formed. The clear filtrate solution was concentrated under reduced pressure to yield pure **5** mixed with triphenylphosphane oxide (ca. 15%). The product was used as such, the triphenylphosphane oxide being eliminated in the next step. Alternatively, **5** can be purified by chromatography (SiO_2, CH_2Cl_2/MeOH 100 to, 95:5), but then the yield is low (20%), as a result of partial hydrolysis of the ester moieties, the carboxylic acid product being retained on the column. ^1H NMR ($CDCl_3$, 400 MHz): δ = 7.79 (s, 2 H, H_{ar}), 7.42 (m, 1 H, H_{ar}), 6.86 (m, 1 H, H_{ar}), 6.82 (m, 1 H, H_{ar}), 6.14 (m, 1 H, H_{ar}), 4.96 (m, 2 H, -CH_2-), 4.45 (m, 2 H, -CH_2), 4.30 (m, 2 H, -CH_2-), 4.18 (m, 4 H, -CH_2-), 3.89 (m, 4 H, -CH_2-), 3.75 (s, 2 H, -CH_3), 2.38 (s, 3 H, -CH_3), 1.44 (t, J = 7.1 Hz, 6 H, -CH_3) ppm.

4-[(4-Methylcoumarin-7-yl)oxypolyoxyethylenyl]dipicolinic Acid (H_2DPApC): To a solution of crude product **5** (0.81 mmol, 0.43 g) in EtOH (20 mL) was added dropwise an aqueous solution of NaOH (0.5 M, 1.77 mmol, 3.54 mL), and the solution was stirred at room temperature for 20 min. The solvent was then evaporated under reduced pressure, and the aqueous solution was washed three times with CH_2Cl_2 (3 × 50 mL) to remove triphenylphosphane oxide. It was acidified with HCl (1 M) down to pH 1.5. The acidic solution was then extracted three times with CH_2Cl_2 (3 × 150 mL), the organic phase was dried with Na_2SO_4, filtered, and concentrated under reduced pressure to yield H_2DPApC (315 mg, 85% over two steps) as a white powder. ^1H NMR (D_2O, 400 MHz): δ = 7.43 (s, 2 H, H_{ar}), 7.36 (m, 1 H, H_{ar}), 6.78 (m, 1 H, H_{ar}), 6.70 (m, 1 H, H_{ar}), 6.02 (m, 1 H, H_{ar}), 4.27 (d, J = 0.8 Hz, 2 H, -CH_2-), 4.16 (m, 2 H, -CH_2-), 3.97 (m, 2 H, -CH_2-), 3.93 (m, 2 H, -CH_2-), 3.84 (m, 4 H, -CH_2-), 2.20 (s, 3 H, CH_3) ppm. $C_{23}H_{23}NO_{10}$·1.6H_2O (502.26): calcd. C 55.00, H 5.26, N 2.79; found C 55.07, H 5.23, N 3.04.

Tris(4-[(4-methylcoumarin-7-yl)oxypolyoxyethylenyl]dipicolinato)-europium {$Cs_3[Eu(DPApC)_3]^{3-}$}: Solid H_2DPApC (0.53 g, 1.12 mmol) was mixed with solid Eu_2O_3 (0.17, 0.48 mmol) and stirred in refluxed H_2O (5 mL) for 30 min. Cs_2CO_3 (0.53 g, 1.62 mmol) was then added to the hot solution. When necessary, additional cesium carbonate was added to obtain a clear solution. The solution was then filtered and kept at room temperature overnight. No crystallization was observed. The solvent was evaporated under reduced pressure until the formation of an oily aggregate. This aggregate then formed a vitrified solid (small beads) when left to dry in air. Further drying was needed under reduced pressure to yield $Cs_3[Eu(DPApC)_3]$ as a yellow to orange solid. $Cs_3C_{69}H_{63}EuN_3O_{30}$·4$H_2O$ (2037.01): calcd. C 40.69, H 3.51, N 2.06; found C 40.70, H 3.24, N 2.15.

Supporting Information (see footnote on the first page of this article): ESI-TOF-MS analysis of the complex, UV/Vis absorption upon Eu^{3+} addition, europium emission compared to similar complexes, CpOMe absorption and excitation spectra, peak fitting of the coumarin extinction coefficient as a function of wavenumber, ratio of coumarin and europium emission in solution and in the solid state, excitation spectra for the emission of europium and coumarin in the solid state and ratio of coumarin to europium emission relative to excitation at 320 nm, calculated molecular orbitals of CpOMe and DPApOMe, quantum yields for the europium and coumarin emission in different solvent mixtures, corrected excitation spectra of the pure and mixed-ligand complexes, Stern–Volmer plot for the emission of europium and coumarin with increasing ratio of DPApC ligand.

Acknowledgments

We thank Jean-Claude G. Bünzli for hosting us in his laboratory, Frédéric Gumy and Svetlana Eliseeva for high-resolution excitation measurements, and Roger D. Hersch for providing financial support. This research is supported through grants from the Swiss National Science foundation (FNS 126757).

[1] I. Grenthe, *J. Am. Chem. Soc.* **1961**, *83*, 360–364.
[2] I. Grenthe, I. Tobiasson, *Acta Chem. Scand.* **1963**, *17*, 2101–2101.
[3] A. Mondry, P. Starynowicz, *J. Alloys Compd.* **1995**, *225*, 367–371.
[4] P. A. Brayshaw, J.-C. G. Bünzli, P. Froidevaux, J. M. Harrowfield, Y. Kim, A. N. Sobolev, *Inorg. Chem.* **1995**, *34*, 2068–2076.
[5] P. A. Brayshaw, J. M. Harrowfield, A. N. Sobolev, *Acta Crystallogr., Sect. C: Cryst. Struct. Commun.* **1995**, *51*, 1799–1802.
[6] J. M. Harrowfield, Y. Kim, B. W. Skelton, A. H. White, *Aust. J. Chem.* **1995**, *48*, 807–823.
[7] H. Donato, R. B. Martin, *J. Am. Chem. Soc.* **1972**, *94*, 4129–4131.
[8] C. N. Reilley, B. W. Good, J. F. Desreux, *Anal. Chem.* **1975**, *47*, 2110–2116.
[9] C. Platas, C. Piguet, N. André, J.-C. G. Bünzli, *J. Chem. Soc., Dalton Trans.* **2001**, 3084–3091.
[10] N. Ouali, B. Bocquet, S. Rigault, P.-Y. Morgantini, J. Weber, C. Piguet, *Inorg. Chem.* **2002**, *41*, 1436–1445.
[11] A.-S. Chauvin, F. Gumy, D. Imbert, J.-C. G. Bünzli, *Spectrosc. Lett.* **2004**, *37*, 517; erratum: A.-S. Chauvin, F. Gumy, D. Imbert, J.-C. G. Bünzli, *Spectrosc. Lett.* **2006**, *40*, 193.
[12] F. G. Prendergast, J. Lu, P. J. Callahan, *J. Biol. Chem.* **1983**, *258*, 4075–4078.
[13] A. Aebischer, F. Gumy, J.-C. G. Bünzli, *Phys. Chem. Chem. Phys.* **2009**, *11*, 1346–1353.
[14] J. B. Lamture, Z. H. Zhou, A. S. Kumar, T. G. Wensel, *Inorg. Chem.* **1995**, *34*, 864–869.
[15] X.-H. Yin, M. Y. Tan, *Zhongguo Xitu Xuebao (J. Chin. Rare Earth Soc.)* **2001**, *19*, 555–560.
[16] X.-H. Yin, M. Y. Yang, H. H. Shi, G. Yang, X. B. Chen, L.-Q. Gu, *Zhongguo Xitu Xuebao (J. Chin. Rare Earth Soc.)* **2000**, *18*, 211–214.
[17] M. W. George, C. A. Golden, M. C. Grossel, R. J. Curry, *Inorg. Chem.* **2006**, *45*, 1739–1744.
[18] A.-L. Gassner, C. Duhot, J.-C. G. Bünzli, A.-S. Chauvin, *Inorg. Chem.* **2008**, *47*, 7802–7812.
[19] M. Latva, H. Takalo, V. M. Mukkala, C. Matachescu, J.-C. Rodriguez-Ubis, J. Kankare, *J. Lumin.* **1997**, *75*, 149–169.
[20] K. Binnemans, *Chem. Rev.* **2009**, *109*, 4283–4374.
[21] N. M. Shavaleev, S. V. Eliseeva, R. Scopelliti, J.-C. G. Bünzli, *Chem. Eur. J.* **2009**, *15*, 10790–10802.
[22] W. Yang, J. Z. Gao, M. Chen, J. W. Kang, *Spectrosc. Lett.* **1997**, *30*, 367–378.
[23] C. Reinhard, H. U. Güdel, *Inorg. Chem.* **2002**, *41*, 1048–1055.
[24] D. C. Lai, B. Dunn, J. I. Zink, *Inorg. Chem.* **1996**, *35*, 2152–2154.
[25] P. C. R. Soares-Santos, H. I. S. Nogueira, V. Felix, M. G. B. Drew, R. A. S. Ferreira, L. D. Carlos, T. Trindade, *Chem. Mater.* **2003**, *15*, 100–108.
[26] P. M. Pellegrino, N. F. Fell, D. L. Rosen, J. B. Gillespie, *Anal. Chem.* **1998**, *70*, 1755–1760.
[27] M. L. Cable, J. P. Kirby, K. Sorasaenee, H. B. Gray, A. Ponce, *J. Am. Chem. Soc.* **2007**, *129*, 1474–1475.
[28] J. P. Kirby, K. J. Venkateswaran, A. Ponce, **2007**, USA.
[29] T. D. Barela, A. D. Sherry, *Anal. Biochem.* **1976**, *71*, 351–357.
[30] N. Tancrez, C. Feuvrie, I. Ledoux, J. Zyss, L. Toupet, H. Le Bozec, O. Maury, *J. Am. Chem. Soc.* **2005**, *127*, 13474–13475.

[31] H. Hou, Y. Wei, Y. Song, Y. Fan, Y. Zhu, *Inorg. Chem.* **2004**, *43*, 1323–1327.
[32] A. D′Aléo, G. Pompidor, B. Elena, J. Vicat, P. L. Baldeck, L. Toupet, R. Kahn, C. Andraud, O. Maury, *ChemPhysChem* **2007**, *8*, 2125–2132.
[33] A. Picot, F. Malvolti, B. LeGuennic, P. L. Baldeck, J. A. G. Williams, C. Andraud, O. Maury, *Inorg. Chem.* **2007**, *46*, 2659–2665.
[34] A. Picot, A. D′Aleo, P. L. Baldeck, A. Grichine, A. Duperray, C. Andraud, O. Maury, *J. Am. Chem. Soc.* **2008**, *130*, 1532–1533.
[35] A.-S. Chauvin, S. Comby, B. Song, C. D. B. Vandevyver, J.-C. G. Bünzli, *Chem. Eur. J.* **2008**, *14*, 1726–1739.
[36] P. Hammond, A. Fletcher, R. Henry, R. Atkins, *Applied Physics A: Mater. Science Process.* **1975**, *8*, 311–314.
[37] D. P. Specht, P. A. Martic, S. Farid, *Tetrahedron* **1982**, *38*, 1203–1211.
[38] B. D. Wagner, *Molecules* **2009**, *14*, 210–237.
[39] R. M. Supkowski, W. d. Horrocks Jr., *Inorg. Chim. Acta* **2002**, *340*, 44–48.
[40] T. Moriya, *Bull. Chem. Soc. Jpn.* **1983**, *56*, 6–14.
[41] F. Gumy, PCT/IB2007/054187, **2009**.
[42] S. Tobita, M. Arakawa, I. Tanaka, *J. Phys. Chem.* **1984**, *88*, 2697–2702.
[43] S. Tobita, M. Arakawa, I. Tanaka, *J. Phys. Chem.* **1985**, *89*, 5649–5654.
[44] *Scigress Explorer Ultra 7.7.0.47*, Fujitsu Limited, **2007**.
[45] A. B. Pangborn, M. A. Giardello, R. H. Grubbs, R. K. Rosen, F. J. Timmers, *Organometallics* **1996**, *15*, 1518–1520.
[46] G. Schwarzenbach, *Complexometric Titrations*, Chapman & Hall, London, **1957**.
[47] H. Gampp, M. Maeder, C. J. Meyer, A. D. Zuberbühler, *Talanta* **1985**, *23*, 1133–1139.
[48] M. H. V. Werts, R. T. F. Jukes, J. W. Verhoeven, *Phys. Chem. Chem. Phys.* **2002**, *4*, 1542–1548.
[49] A. Cappelli, S. Galeazzi, M. Anzini, S. Vomero, PCT/EP2007/059698, **2008**.

Received: February 3, 2010
Published Online: ■

